where

$$[H] = \int_{V_m} [R]^T[C][R]dV \tag{12}$$

$$\{F_1\} = 2\int_{V_m} [R]^T[C]\{R_2\}dV + \int_{S_{u_m}} T_i\bar{u}_i$$

$$\lfloor \alpha \rfloor[P]\{\beta\} + \lfloor \beta \rfloor\{F_2\} = \int_{\partial V_m} \lfloor T_i \rfloor\{u_{Li}\}dS \tag{13}$$

$$\lfloor \beta \rfloor[G]\{Q\} = \int_{\partial V_m} \lfloor u_{Li} \rfloor\{\bar{T}_i\}dS \tag{14}$$

and C_m is a constant. In the above $[C]$ is the elasticity compliance matrix. Since only the parameters $\{\alpha\}$ and $\{\beta\}$ are independent for each element, taking the variation of Eq. (1) with respect to $\{\alpha\}$ and $\{\beta\}$, leads to the Euler equations for each element, as

$$-[H]\{\alpha\} - \{F_1\} + [P]\{\beta\} = 0 \tag{15}$$

and

$$[P]^T\{\alpha\} + \{F_2\} - [G]\{Q\} = 0 \tag{16}$$

From Eqs. (15) and (16) one can solve for $\{\alpha\}$ and $\{\beta\}$ as,

$$\{\alpha\} = +[H]^{-1}[P]\{\beta\} - [H]^{-1}\{F_1\} \tag{17}$$

and

$$\{\beta\} = ([P]^T[H]^{-1}[P])^{-1}[G]\{Q\} + ([P]^T[H]^{-1}[P])^{-1}([P]^T[H]^{-1}\{F_1\} - \{F_2\}) \tag{18}$$

It can be seen from the above equations that the number of α's must be larger or equal to the number of β's and the rank of $[P]$ equal to the number of β's in order to have $\{\beta\}$ and $\{\alpha\}$ solvable in terms of $\{Q\}$. Substituting Eqs. (17) and (18) in Eq. (11), one can express π_F in terms of $\{Q\}$ alone, as,

$$\pi_F = +\Sigma_m (+\tfrac{1}{2}Q[D_m]\{Q\} - Q\{E_m\} + C_m^*) \tag{19}$$

where

$$[D_m] = [G]^T([P]^T[H]^{-1}[P])^{-1T}[G] \tag{20}$$

$$\{E_m\} = [G]^T([P]^T[H]^{-1}[P])^{-1T} \times (-[P]^T[H]^{-1}\{F_1\} + \{F_2\}) \tag{21}$$

The matrix $[D_m]$ is symmetric and positive definite because $[H]$ is symmetric and positive definite and the rank of $[P]$ is equal to the number of β's. Using the generalized nodal forces $\{Q^*\}$ for the finite-element assembly, and since these can be subjected to independent variation, one obtains a final set of equations of the form

$$[D]\{Q^*\} = [E] \tag{22}$$

In Eqs. (20) and (21), in order to form $[D_m]$ and $[E_m]$, matrix inversions have to be performed twice. But, if there are as many β's as α's, it can be seen from Eq. (13) that the matrix $[P]$ becomes square. Hence,

$$(P^TH^{-1}P)^{-1} = [P]^{-1}[H][P^T]^{-1} \tag{23}$$

Thus, the expressions for $[D_m]$ and $[E_m]$ can be simplified as

$$[D_m] = [G]^T[P^{-1}][H][P]^{-1T}[G] \tag{24}$$

and

$$\{E_m\} = -G^T[P^{-1}]^T\{F_1\} + [G]^T[P]^{-1}[H][P]^{-1T}\{F_2\} \tag{25}$$

Closure

Unlike in the equilibrium stress model of de Veubeke and Sander,[4] and the hybrid stress model of Pian,[5] the unknowns in the final set of matrix equations for the finite-element assembly in the present assumed stress model are the nodal values of stresses. Thus, stress boundary conditions can be handled more conveniently. This is of advantage in problems such as analysis of stress-states around holes in plane-stress problems, stress-states around cut-outs in shells, and stress-states in plates with extending cracks, where stress-free boundary conditions have to be satisfied. Also, since the stress-states at node points are directly solved for, it is very convenient to apply the yield criteria and flow rules in plasticity problems. The use of the method in such problems is currently being investigated. It should be pointed out that this method is a direct analogy of the hybrid displacement model used by Tong,[3] and the author.[2]

References

[1] Pian, T. H. H. and Tong, P., "Basis of Finite Element Methods for Solid Continua," *International Journal of Numerical Methods in Engineering*, Vol. 1, 1969, pp. 3–28.

[2] Atluri, S., "Static Analysis of Shells of Revolution Using Doubly-Curved Quadrilateral Elements Derived From Alternate Variational Models," SAMSO TR 69-394, June 1969, Norton Air Force Base, Calif., pp. 27–76.

[3] Tong, P., "New Displacement Hybrid Finite Element for Solid Continua," *International Journal of Numerical Methods in Engineering*, Vol. 2, 1970, pp. 73–83.

[4] Fraejis de Veubeke and Sander, G., "An Equilibrium Model for Plate Bending," *International Journal of Solids and Structures*, Vol. 4, 1968, pp. 447–468.

[5] Pian, T. H. H., "Element Stiffness Matrices for Boundary Compatibility and for Prescribed Boundary Stresses," *Proceedings of the Conference on Matrix Methods in Structural Mechanics*, AFFDL TR-66-80, 1965, pp. 457–477.

[6] Kobayashi, A. R., Chiu, S. T. and Beeukes, R., "Elastic-Plastic State in a Plate with an Extended Crack," *Proceedings of the 1970 U.S. Army Conference on Solid Mechanics-Light Weight Structures*, to be published.

[7] Hu, H. C., "On Some Variational Principles in the Theory of Elasticity and Plasticity," *Scintia Sinica*, Vol. 4, No. 1, March 1955, pp. 33–54.

[8] Washizu, K., *Variational Methods in Elasticity and Plasticity*, Pergamon, New York, 1968, pp. 27–51.

An Effective Approximation for Computing the Three-Dimensional Laminar Boundary-Layer Flows

KENNETH K. WANG*

McDonnell Douglas Astronautics Company, Huntington Beach, Calif.

Nomenclature

c	=	density-viscosity ratio, $\rho\mu/\rho_w\mu_w$
f	=	$\int_o^\eta Fd\eta$
F	=	u/u_e
g	=	$\int_o^\eta Gd\eta$
G	=	v/u_e
H	=	total enthalpy
K_1	=	curvature, streamwise
K_2	=	curvature, orthogonal to streamline
Pr	=	Prandtl number
S_1,S_2,S_3	=	curvilinear coordinates in the stream wise, crossflow and normal directions
u,w,v	=	velocity components in the S_1,S_2, and S_3 directions
ρ	=	density
μ	=	viscosity
ξ,ζ,η	=	transformed coordinates

Received October 16, 1970; revision received April 29, 1971. This work was supported by the McDonnell Douglas Astronautics Company Independent Research and Development (IRAD) program.

Index Category: Boundary Layers and Convective Heat Transfer—Laminar.

* Senior Engineer/Scientist, Aero/Thermodynamics and Nuclear Effects Department.

Subscripts

w = value at wall
e = value at boundary-layer edge

IN treating three-dimensional, laminar, compressible boundary-layer flow, various approaches have been employed in the past in an effort to reduce complexity and thereby render solution possible. Well-known methods such as the integral method,[1] similar solution[2] and small cross flow perturbation[3] have been used with varying degree of success. With the recent interest in the development of arbitrary configuration, e.g., space shuttle vehicles, it appears that a solution with less restrictive approach will be desirable, particularly, to avoid the large computing time required for exact numerical solution.[4]

A well-recognized fact utilized[5] in past investigations is that the laminar boundary layer can be approximated by division into two regions of distinct physical behavior; region (1), the neighborhood of the wall where viscous stress dominates the flow, and region (2), the outer portion of the boundary layer which retains much the characteristics of the inviscid flow. In a recent paper, Vaglio-Laurin and Miller[6] employed the two region model to formulate a set of governing differential equations specialized for each region. Analytic solutions were derived and compared with the exact result[2] for flow near the plane of symmetry. In the present paper, with the emphasis on numerical computations, this physical description of the flow is employed in constructing an effective approximation which facilitates the numerical solution of the governing equations.

To proceed with the analysis, the governing equations for the flow are written in a curvilinear coordinate system aligned along the inviscid streamline at the edge of boundary layer.[7] Applying the Howarth-Dorodnitsyn transform

$$\xi = \int \rho_w \mu_w u_e dS_1,\ \zeta = S_2,\ \eta = u_e(2\xi)^{-1/2}\int \rho dS_3$$

and introducing stream functions f and g

$$u = u_e F$$

$$v = u_e G$$

$$\rho w = -K_1 g(2\xi)^{1/2} - K_2 f(2\xi)^{1/2} - \partial/\partial S_1[f(2\xi)^{1/2}] - \partial/\partial S_2[g(2\xi)^{1/2}]$$

the governing equations are

Momentum (streamwise)

$$\frac{\partial}{\partial\eta}\left[C\frac{\partial F}{\partial\eta}\right] + f\frac{\partial F}{\partial\eta} - 2\xi\left[\frac{\partial F}{\partial\xi} - \frac{\partial f}{\partial\xi}\frac{\partial F}{\partial\eta}\right] - \frac{2\xi}{u_e}\frac{\partial u_e}{\partial\xi}\left[F^2 - \frac{\rho_e}{\rho}\right] = 2\xi\left\{K_1\left[FG - g\frac{\partial F}{\partial\eta}\right] - K_2\left[f\frac{\partial F}{\partial\eta} + G^2\right] - \frac{G}{u_e}\frac{\partial u}{\partial\zeta} - \frac{\partial g}{\partial\zeta}\frac{\partial F}{\partial\eta}\right\}(\rho_w\mu_w u_e)^{-1} \quad (1)$$

Momentum (crossflow)

$$\frac{\partial}{\partial\eta}\left[C\frac{\partial G}{\partial\eta}\right] + f\frac{\partial G}{\partial\eta} - 2\xi\left[\frac{F}{u_e}\frac{\partial}{\partial\xi}(u_e G) - \frac{\partial f}{\partial\xi}\frac{\partial G}{\partial\eta}\right] = 2\xi\left\{-K_1\left[F^2 - \frac{\rho_e}{\rho} + g\frac{\partial G}{\partial\eta}\right] + K_2\left[FG - f\frac{\partial G}{\partial\eta}\right] - \frac{G}{u_e}\frac{\partial v}{\partial\zeta} + \frac{\partial g}{\partial\zeta}\frac{\partial G}{\partial\eta}\right\}(\rho_w\mu_w u_e)^{-1} \quad (2)$$

Energy

$$\frac{\partial}{\partial\eta}\left[\frac{C}{Pr}\frac{\partial H}{\partial\eta}\right] + 2\xi\left\{\frac{f}{2\xi} + \frac{\partial f}{\partial\xi} + \left[\frac{\partial g}{\partial\zeta} + K_1 g + K_2 f\right]\times(\rho_w\mu_w u_e)^{-1}\right\}\frac{\partial H}{\partial\eta} - 2\xi\left[F\frac{\partial H}{\partial\xi} + G\frac{\partial H}{\partial\zeta}(\rho_w\mu_w u_e)^{-1}\right] + \frac{\partial}{\partial\eta}\left[\left(C - \frac{C}{Pr}\right)\frac{\partial}{\partial\eta}(u^2 + v^2)\right] = 0 \quad (3)$$

with the boundary conditions at $\eta = 0$, $F = f = G = g = 0$, $H = H_w$ and at $\eta = \infty$, $F = 1$, $G = 0$, $H = H_e$.

A major difficulty in obtaining solutions to the above equations is the presence of terms containing a derivative in the crossflow direction, i.e., the ζ derivative. Their existence requires the consideration of a three-dimensional domain and consequently, the computational effort in obtaining a numerical solution can be expected to increase greatly over that of the two-dimensional case. Past effort at removing this obstacle generally have relied on either the restrictions of crossflow magnitude or similarity conditions. In considering the different physical behavior in the aforementioned regions it is suggested here that the terms be approximated by their values at the edge of inviscid flow. This approach is justified by the following reasoning. In region (2) the flow retains largely its inviscid character, and thus the approximation can be expected to be good there. On the other hand, the terms in question contribute little to the flow in region (1) where the viscous effect dominate. Their approximation therefore will not cause large errors in region (1). Consequently for subsequent numerical computations, the following relations will be used:

$$G\partial u/\partial\zeta \sim G\partial u_e/\partial\zeta,\ G\partial v/\partial\zeta \sim G\partial v_e/\partial\zeta,\ \partial g/\partial\zeta = 0,\ G\partial H/\partial\zeta \sim G\partial H_e/\partial\zeta \quad (4)$$

Note that, in addition to being exact at the edge of boundary layer, they also satisfy the required values at the wall.

The use of this approximation yields certain advantages. Notably, the computing effort can be expected to be drastically reduced. This can be seen by observing that the governing equations now have only the ξ (streamwise) and η (normal) derivatives. Mathematically, they can be integrated numerically along any inviscid streamline using the

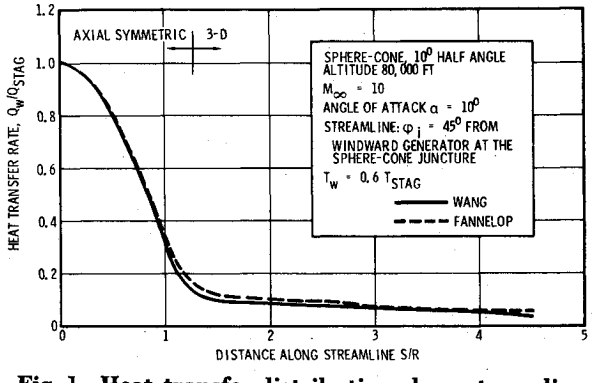

Fig. 1 Heat-transfer distribution along streamline.

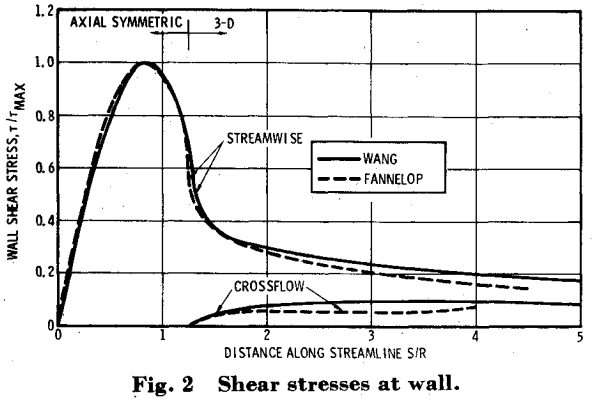

Fig. 2 Shear stresses at wall.

conventional schemes such as those successfully used in solving the two-dimensional boundary-layer flows, thus avoiding the large computing time required for the exact solution. Additionally, the numerical solution is basically less restrictive in view of the nature of the approximations as compared with the existing methods.[1,3] As this physical model is valid wherever the boundary-layer concept is applicable, present approximations should be effective for a wide class of vehicle geometries and flow conditions. With the governing equations written in central difference form and using the Crank-Nicholson type of implicit schemes, they have been programmed for numerical calculation.

For comparative purposes, the case presented in Ref. 3 was selected. It is seen that the heat-transfer rates as shown in Fig. 1 correspond very well considering the difference in the inviscid result used (Newtonian vs linear characteristic) and the streamline curvature computations (exact vs approximate). The shear stress in the streamwise and the crossflow directions similarly show good agreement as indicated in Fig. 2. However, the present calculation shows a definite maxima in the crossflow shear stress near $S/R = 4$. Available oil streak experimental results[8,11] appear to favor the trend as predicted by the present calculation. Future computations using exact inviscid inputs[9,10] will be needed to provide credence to this point of view.

In summary, an approximation based on a physical description of the boundary-layer flow has been devised. Its use has greatly simplified the task of numerical integration of the governing equations of three-dimensional, compressible laminar boundary layer. Numerical results have validated the effectiveness of the approximation and the computing time (to $S/R = 10$) per case ($\sim$2 min on CDC 6500) appears to be reasonable.

References

[1] Kang, S. W., Rae, W. J., and Dunn, M. G., "Effects of Mass Injection on Compressible, Three-Dimensional Laminar Boundary Layers," *AIAA Journal*, Vol. 5, No. 10, Oct. 1967, pp. 1738–1745.

[2] Trella, M. and Libby, P. A., "Similar Solutions for the Hypersonic Laminar Boundary Layer Near a Plane of Symmetry," *AIAA Journal*, Vol. 3, No. 1, Jan. 1965, pp. 75–83.

[3] Fannelop, T. K., "A Method of Solving the Three-Dimensional Laminar Boundary Layer Equations with Application to a Lifting Reentry Body," *AIAA Journal*, Vol. 6, No. 6, June 1968, pp. 1075–1084.

[4] Der, J., Jr. and Raetz, G. S., "Solution of General Three-Dimensional Laminar Boundary Layer Problem by an Exact Numerical Method," IAS Paper 62-70, Jan. 1962.

[5] Stewartson, K., "Viscous Hypersonic Flow Past a Slender Cone," *The Physics of Fluids*, Vol. 7, No. 5, May 1964, pp. 667–675.

[6] Vaglio-Laurin, R. and Miller, G., "On Three-Dimensional Laminar Boundary Layers with Large Cross-Flow," *AIAA Journal*, Vol. 8, No. 10, Oct. 1970, pp. 1822–1830.

[7] Mayer, A., "Three-Dimensional Laminar Boundary Layers," *High Speed Aero/Dynamics and Jet Propulsion*, Vol. IV, Princeton University Press, Princeton, N.J., 1964, pp. 288–292.

[8] Rainbird, W. J., Crabbe, R. S., and Jurewicz, "A Water Tunnel Investigation of the Flow Separation About Circular Cones at Incidence," LR-385, Sept. 1963, National Research Council of Canada, Ottawa, Canada.

[9] Jones, D. J., "Numerical Solutions of the Flow Field for Conical Bodies in a Supersonic Stream," LR-507, July 1968, National Research Council of Canada, Ottawa, Canada.

[10] Rakich, V. V. and Cleary, J. W., "Theoretical and Experimental Study of Supersonic Steady Flow Around Inclined Bodies of Revolution," *AIAA Journal*, Vol. 8, No. 3, March 1970, pp. 511–518.

[11] Stetson, K. F. and Friberg, E. G., "Surface Conditions in the Leeward Region of a Blunt Cone at Angle of Attack in Hypersonic Flow," ARL-69-0114, July 1969, ARL, Dayton, Ohio.

Shock Standoff Distances and Mach-Disk Diameters in Underexpanded Sonic Jets

W. Davidor* and S. S. Penner†

University of California, San Diego, La Jolla, Calif.

Nomenclature

d_e = nozzle-exit diameter
d_s = Mach-disk diameter
p = pressure
x = distance downstream of the nozzle-exit location
γ = isobaric to isochoric heat-capacity ratio
ξ = x/d_e

Subscripts

1 = upstream chamber conditions
a = downstream (ambient) conditions

Introduction

A NUMBER of theoretical[1–4] and experimental[1,5–7] studies has been published on the relation between pressure ratio and shock standoff distance. In particular, extensive compilations of experimental measurements have been published by Lewis and Carlson[6] and by Crist, Sherman, and Glass,[7] who noted that the ratio of stagnation pressure (p_1) to ambient pressure (p_a) was proportional to the square of the dimensionless ratio (ξ) of downstream distance (x) divided by the exit diameter (d_e) of a sonic nozzle; the proportionality constant was found[7] to be equal to 2.4 and was independent of the ratio of isobaric to isochoric specific heat (γ).

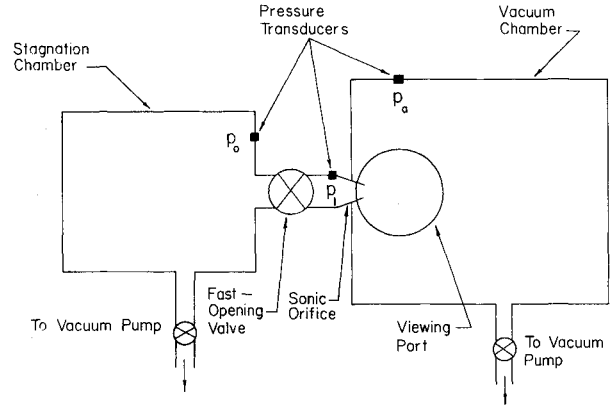

Fig. 1 Schematic diagram of the blow-down tunnel used for determining shock standoff distance as a function of pressure ratio. Volume of stagnation chamber = 524 cm³; volume of vacuum chamber = 7054 cm³; exit diameter of sonic nozzle = 0.680 cm; entrance diameter of sonic nozzle = 2.86 cm; the fast-opening valve is a shock-actuated valve which opens completely in 20 to 25 msec; pressure-transducer readings were accurate to about ±5%. The initial pressure p_1 was between 11.75 and 13.25 psia with $p_a \simeq 0.8$ psia.

Received December 17, 1970; revision received April 12, 1971. These studies have been supported under Project Themis and were sponsored by the Air Force Office of Scientific Research, Office of Aerospace Research, U.S. Air Force, under Contract F44620-68-C-0010. The authors are indebted to K. G. P. Sulzmann for assistance with the experimental studies and for helpful discussions.

* Assistant Research Engineer, Department of the Aerospace and Mechanical Engineering Sciences.

† Professor of Engineering Physics, Department of the Aerospace and Mechanical Engineering Sciences. Fellow AIAA.